Progress In Electromagnetics Research C, Vol. 3, 19–43, 2008

NUMERICAL ANALYSIS OF COMBINED FIELD INTEGRAL EQUATION FORMULATIONS FOR ELECTROMAGNETIC SCATTERING BY DIELECTRIC AND COMPOSITE OBJECTS

P. Ylä-Oijala

Department of Radio Science and Engineering
Helsinki University of Technology
Finland

Abstract—Numerical analysis of a generalized form of the recently developed electric and magnetic current combined field integral equation (JM-CFIE) for electromagnetic scattering by homogeneous dielectric and composite objects is presented. This new formulation contains a similar coupling parameter α as CFIE contains in the case of perfectly conducting objects. Two alternative JM-CFIE(α) formulations are introduced and their numerical properties (solution accuracy and convergence of iterative Krylov subspace methods) are investigated. The properties of these formulations are found to be very sensitive to the choice of α and to the permittivity of the object. By using normalized fields and currents the optimal value of α minimizing the number of iterations becomes only weakly dependent on the permittivity object. Using linear-linear basis functions instead of the more conventional constant-linear (RWG) basis functions the solution accuracy can be made less dependent on the choice of α.

1. INTRODUCTION

Surface integral equation methods are popular in solving electromagnetic scattering and radiation problems containing metallic, homogeneous dielectric and composite materials [1]. One of the desired properties of a surface integral equation formulation is that it eliminates internal resonances. In the case of closed perfectly conducting (PEC) objects this can be achieved, for example, with the combined field integral equation (CFIE) [2]. CFIE (PEC-CFIE) is a well-known linear combination of the electric and magnetic field integral equations (EFIE and MFIE).

In the case of homogeneous dielectric objects there are a lot of formulations, called coupled region integral equations (CRIE) [1, 3], that are free of the internal resonances. Well-known examples of these formulations are Poggio-Miller-Chang-Harrington-Wu-Tsai (PMCHWT) and Müller formulations. In the CRIE formulations the EFIEs and MFIEs of the exterior and interior problems are coupled, but the EFIEs and MFIEs are not usually mixed. Formulations where EFIEs and MFIEs are mixed, i.e., CFIE type formulations, are also possible. However, by directly combining the EFIEs and MFIEs in a similar manner as in the PEC-CFIE [4], yields an unstable formulation [5–7]. As a remedy to this problem, a special testing procedure [5], and a new formulation, electric and magnetic current CFIE (JM-CFIE) [7], have been proposed. CFIEs have also been applied in the case of composite metallic and dielectric objects [7–9].

The usual form of PEC-CFIE contains a coupling parameter α, $0 \leq \alpha \leq 1$. Many studies have indicated that the optimal value of α giving rise to the best conditioned matrix equation is between 0.2 and 0.3, see e.g., [10, 11]. If the surface is sufficiently smooth, by increasing the order of the basis functions the solution accuracy can be made only weakly dependent on the choice of α [11, 12] and the condition of the matrix becomes the sole criterion for the choice of α in PEC-CFIE.

In the case of homogeneous dielectric objects the situation is somewhat different. The permittivity of the object, a parameter that does not appear in the PEC case, has a significant effect on the properties of the formulations [12–17]. In many cases the JM-CFIE formulation has been found to be the most robust one, i.e., its properties are less dependent on the material contrast, frequency and other parameters, in particular, as the complexity or the size of the problem increases [13, 18].

All previous implementations of JM-CFIE, however, consider only the original form [7] corresponding to the case $\alpha = 0.5$. The objective of this paper is to generalize the JM-CFIE formulation by adding a similar coupling parameter α as in PEC-CFIE. To this end two new JM-CFIE(α) formulations are introduced and their numerical properties (solution accuracy and convergence of iterative Krylov subspace methods) are investigated as functions of α, permittivity of the object and mesh density.

Numerical results show that in the case of dielectric and composite metallic and dielectric objects the properties of both new JM-CFIE(α) formulations depend strongly on the permittivity of the object and on the choice of α. In particular, the optimal value of α minimizing the number of iterations is very sensitive to the permittivity. The

optimum value for PEC-CFIE between 0.2 and 0.3 seems to be the optimal one in the case of low contrast objects, and for the first new JM-CFIE(α) formulation, only. This "permittivity instability" is identified as a general problem of integral equations of the second kind. The conditioning of the integral equations of the second kind decreases as the permittivity contrast increases. As a remedy to this problem we propose to use normalized field quantities [16, 19]. With the normalized fields and currents the properties of both new JM-CFIE(α) formulations can be stabilized and the optimal values of α minimizing the number of iterations become only weakly dependent on the permittivity. In addition, we show that, similarly as in the case of PEC-CFIE, by using linear-linear basis functions instead of constant-linear (RWG) functions, the solution accuracy of the new JM-CFIE(α) formulations can be made less dependent on the choice of α.

2. COMBINED FIELD INTEGRAL EQUATIONS

Consider time-harmonic electromagnetic scattering by a homogeneous dielectric object D in a homogeneous medium. The time factor is $e^{-i\omega t}$. Let S denote the surface of D. The exterior and interior of D are denoted by $D_{\rm e}$ and $D_{\rm i}$ and $\varepsilon_{\rm e}$, $\mu_{\rm e}$ and $\varepsilon_{\rm i}$, $\mu_{\rm i}$ are the constant parameters of $D_{\rm e}$ and $D_{\rm i}$, respectively. Vectors $\boldsymbol{n}_{\rm e}$ and $\boldsymbol{n}_{\rm i}$ are the unit normal vectors on S pointing into $D_{\rm e}$ and $D_{\rm i}$.

In the following T-EFIE$_{\rm i}$, T-EFIE$_{\rm e}$, T-MFIE$_{\rm i}$ and T-MFIE$_{\rm e}$ denote the electric and magnetic field integral equations of the interior (i) and exterior (e) regions, respectively. These equations are obtained by taking the tangential components of the surface integral representations of the total electric and magnetic fields on the surface S. N-EFIE$_{\rm i}$, N-EFIE$_{\rm e}$, N-MFIE$_{\rm i}$ and N-MFIE$_{\rm e}$ are the corresponding surface integral equations obtained by operating with $\boldsymbol{n}_{\rm e}\times$ and $\boldsymbol{n}_{\rm i}\times$ to the surface integral representations on S. More details on the derivation of these equations is presented in [13].

In the case of metallic perfectly conducting objects the combined field integral equation (CFIE) is the following linear combination of T-EFIE$_{\rm e}$ and N-MFIE$_{\rm e}$ [2]

$$\alpha\frac{1}{\eta_e}\text{T-EFIE}_{\rm e} + (1-\alpha)\text{N-MFIE}_{\rm e}. \tag{1}$$

Here α, $0 \le \alpha \le 1$, is a coupling parameter and $\eta_{\rm e}$ is the constant wave impedance of the exterior.

In the case of homogeneous dielectric objects the electric and

magnetic current CFIE, JM-CFIE, contains two combined equations [7]

$$\frac{1}{\eta_{\rm i}}\text{T-EFIE}_{\rm i} + \frac{1}{\eta_{\rm e}}\text{T-EFIE}_{\rm e} + \text{N-MFIE}_{\rm i} + \text{N-MFIE}_{\rm e} \tag{2}$$

$$\eta_{\rm i}\text{T-MFIE}_{\rm i} + \eta_{\rm e}\text{T-MFIE}_{\rm e} - \text{N-EFIE}_{\rm i} - \text{N-EFIE}_{\rm e}. \tag{3}$$

Here η_e and η_i are the wave impedances outside and inside the object, respectively.

Next JM-CFIE formulation (2)–(3) is generalized by adding the coupling parameter α, $0 \leq \alpha \leq 1$, similarly as in PEC-CFIE (1). Because JM-CFIE contains two equations, α parameter can be added by two alternative ways, giving rise to two new formulations. The first formulation, denoted in the sequel by JM-CFIE1(α), reads

$$\alpha\Big(\frac{1}{\eta_{\rm i}}\text{T-EFIE}_{\rm i} + \frac{1}{\eta_{\rm e}}\text{T-EFIE}_{\rm e}\Big) + \beta\left(\text{N-MFIE}_{\rm i} + \text{N-MFIE}_{\rm e}\right) \tag{4}$$

$$\alpha\left(\eta_{\rm i}\text{T-MFIE}_{\rm i} + \eta_{\rm e}\text{T-MFIE}_{\rm e}\right) - \beta\left(\text{N-EFIE}_{\rm i} + \text{N-EFIE}_{\rm e}\right), \tag{5}$$

where $\beta = 1 - \alpha$. This formulation shares some important properties of the original JM-CFIE formulation. Firstly, it is a coupled region integral equation having the desired property that it removes the internal resonance problem for all α, $0 \leq \alpha \leq 1$. Secondly, by expressing the operators of the combined system by a two times two matrix, the operators on the diagonal blocks are identical for all α (see Section 4). This is in particular important for the balance and conditioning of the matrix [13].

Alternatively, we may combine the equations as follows

$$\alpha\Big(\frac{1}{\eta_{\rm i}}\text{T-EFIE}_{\rm i} + \frac{1}{\eta_{\rm e}}\text{T-EFIE}_{\rm e}\Big) + \beta\left(\text{N-MFIE}_{\rm i} + \text{N-MFIE}_{\rm e}\right), \tag{6}$$

$$-\alpha\left(\text{N-EFIE}_{\rm i} + \text{N-EFIE}_{\rm e}\right) + \beta\left(\eta_{\rm i}\text{T-MFIE}_{\rm i} + \eta_{\rm e}\text{T-MFIE}_{\rm e}\right). \tag{7}$$

Since at $\alpha = 1$ and $\alpha = 0$ this second formulation, denoted by JM-CFIE2(α), contains only electric field integral equations T-EFIE and N-EFIE, or magnetic field integral equations T-MFIE and N-MFIE, respectively, it does not eliminate internal resonances for all α. In addition, the operators on the diagonal of the two times two matrix representation are identical only if $\alpha = 0.5$. Hence, JM-CFIE2(α) is not expected to be as well balanced as JM-CFIE1(α).

For composite metallic and dielectric objects combined CFIE/JM-CFIE formulations are obtained by combining (1) with (4)–(5) or with (6)–(7).

3. ITERATION CONVERGENCE OF JM-CFIE(α) FORMULATIONS

Next the convergence of the iterative solutions of the new JM-CFIE(α) formulations are investigated as a function of α. The equations are discretized using Galerkin's method with Rao-Wilton-Glisson (RWG) [20] functions with planar triangular elements. Iterative solutions are found by the Generalized Minimum Residual (GMRES) method without restarting and preconditioning.

3.1. Homogeneous Dielectric Cube

As a first test case consider electromagnetic scattering by a homogeneous dielectric cube with the side length $\lambda_e/2$, where λ_e is the wavelength in the exterior (vacuum). The center of the cube is at the origin and the faces of the cube are parallel to the x, y and z coordinate axes. Incident wave is an y polarized plane wave propagating along the negative z axis. A cube is chosen because the solution accuracy of some formulations is sensitive to the sharp wedges and corners [12, 13] and discretization error due to modelling of curved surface, a sphere, for example, with planar elements can be avoided.

Figures 1 and 2 show the number of GMRES iterations of the new JM-CFIE(α) formulations as functions of α for a dielectric cube with different permittivities. For JM-CFIE1(α) the value of α minimizing the number of iterations seems to be close to the PEC-CFIE optimal value 0.2–0.3 only at low permittivities. As the permittivity of the cube is increased the optimal value approaches 0.8. In JM-CFIE2(α) the situation is almost opposite and the optimal value of α seems to move from 0.5 to 0.2 as the permittivity of the cube is increased. In particular, in both cases a unique optimum α minimizing the iteration count for all permittivities does not exist.

3.2. Inhomogeneous Dielectric Cube

As a next example consider a piece-wise homogeneous dielectric cube made of two homogeneous boxes. The boxes are of the same size and the interface between them is at the $z = 0$ plane. The relative permittivity of the first box above $z = 0$ is 2 and the relative permittivity of the second box below $z = 0$ is varied from 4 to 40.

Figures 3 and 4 show the number of GMRES iterations of the new JM-CFIE(α) formulations as functions of α. Now the optimum α seems to be less dependent on the permittivity as in the case of a homogeneous cube. In particular, for the JM-CFIE2(α) formulation the optimum seems to be close to 0.5 for all permittivities.

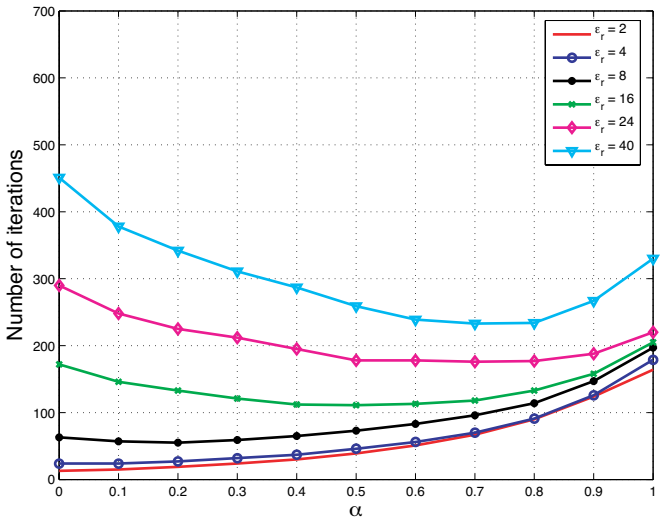

Figure 1. Number of GMRES iterations of JM-CFIE1(α) formulation for a dielectric cube with $\varepsilon_r = 2, \ldots, 40$. The element size $\Delta = \lambda_e/20$ and the number of RWG unknowns is 3600.

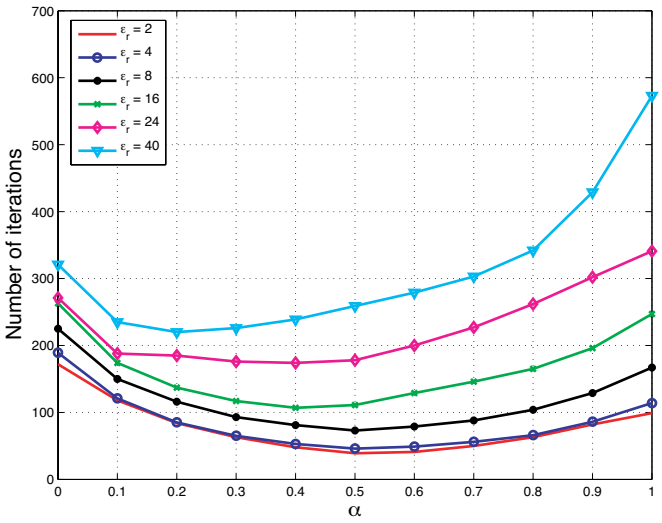

Figure 2. Number of GMRES iterations of JM-CFIE2(α) formulation similarly as in Fig. 1.

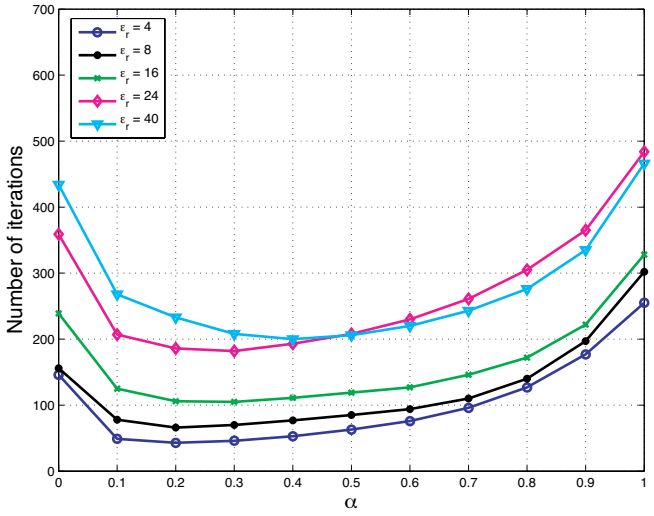

Figure 3. Number of GMRES iterations of JM-CFIE1(α) formulation for a piecewise homogeneous dielectric cube with $\varepsilon_{r1} = 2$ and $\varepsilon_{r2} = 4, \ldots, 40$. The element size $\Delta = \lambda_e/16$ and the number of RWG unknowns is 4192.

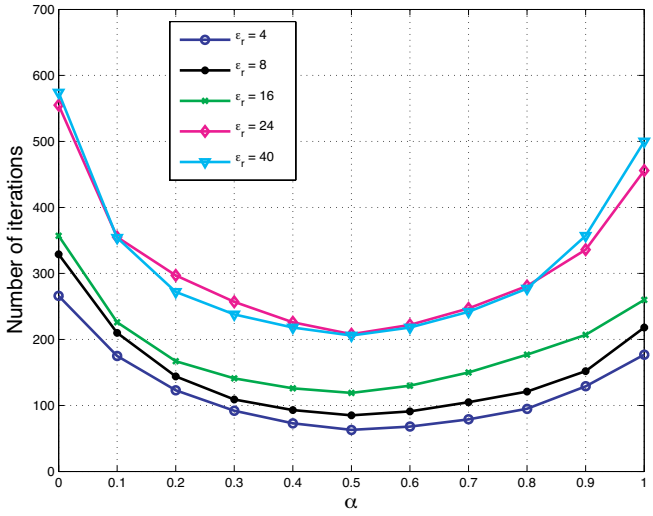

Figure 4. Number of GMRES iterations of JM-CFIE2(α) formulation similarly as in Fig. 3.

3.3. Composite Metallic and Dielectric Cube

As a third example consider a composite metallic and dielectric cube made of two homogeneous boxes of the same size. The first box above $z = 0$ is metallic (PEC) and the second one below $z = 0$ is dielectric with $\varepsilon_r = 2, \ldots, 40$. The incident wave is the same as in the previous examples.

Figures 5 and 6 show the number of GMRES iterations of the new JM-CFIE(α) formulations as functions of α. The results are rather similar as in the case of a piece-wise homogeneous dielectric cube.

4. PERMITTIVITY INSTABILITY OF JM-CFIE(α)

The results of the previous section show that the properties of the new JM-CFIE(α) formulations depend on the permittivity of the object. In particular, the optimum α minimizing the number of iterations is in many cases found to be very sensitive of the permittivity. In this section this "permittivity instability" is studied more carefully.

Let us first introduce the following CFIE operators

$$\boldsymbol{\mathcal{C}}^{\mathrm{e/i}}_{\alpha,\beta}(\boldsymbol{F})(\boldsymbol{r}) = \left(\alpha(\boldsymbol{\mathcal{L}}_{\mathrm{e/i}})_{\tan} + \beta\boldsymbol{n}\times\boldsymbol{\mathcal{K}}_{\mathrm{e/i}} - \beta\Omega\boldsymbol{\mathcal{I}}\right)(\boldsymbol{F})(\boldsymbol{r}) \tag{8}$$

where $\boldsymbol{\mathcal{L}}_{\mathrm{e/i}}$ and $\boldsymbol{\mathcal{K}}_{\mathrm{e/i}}$ are the EFIE and MFIE integral operators of the exterior (e) and interior (i), defined as,

$$\boldsymbol{\mathcal{L}}_{\mathrm{e/i}}(\boldsymbol{F})(\boldsymbol{r}) = \frac{-1}{ik_{\mathrm{e/i}}}\nabla\boldsymbol{\mathcal{S}}_{\mathrm{e/i}}(\nabla_s\cdot\boldsymbol{F})(\boldsymbol{r}) + ik_{\mathrm{e/i}}\boldsymbol{\mathcal{S}}_{\mathrm{e/i}}(\boldsymbol{F}) \tag{9}$$

$$\boldsymbol{\mathcal{K}}_{\mathrm{e/i}}(\boldsymbol{F})(\boldsymbol{r}) = \nabla\times\boldsymbol{\mathcal{S}}_{\mathrm{e/i}}(\boldsymbol{F})(\boldsymbol{r}), \tag{10}$$

$\boldsymbol{\mathcal{S}}_{\mathrm{e/i}}$ is the single-layer integral operator

$$\boldsymbol{\mathcal{S}}_{\mathrm{e/i}}(\boldsymbol{F})(\boldsymbol{r}) = \int_S G_{\mathrm{e/i}}(\boldsymbol{r},\boldsymbol{r}')\boldsymbol{F}(\boldsymbol{r}')dS' \tag{11}$$

with the homogeneous space Green's function $G_{\mathrm{e/i}}$ of the exterior and interior, respectively. In addition, $\boldsymbol{\mathcal{I}}$ is the identity operator, Ω is the relative solid angle and $k_{\mathrm{e/i}}$ is the wavenumber of the exterior (e) and interior (i).

Equations (12) and (13) show the integral operators of JM-

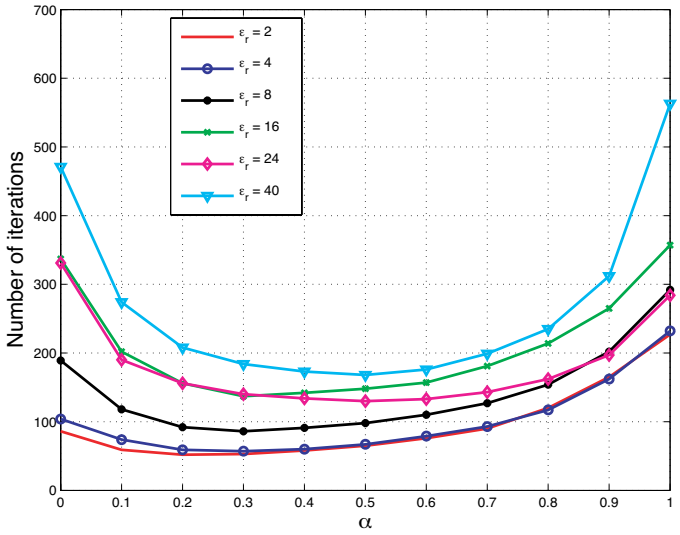

Figure 5. Number of GMRES iterations of JM-CFIE1(α) formulation for a composite metallic and dielectric cube with $\varepsilon_r = 2, \ldots, 40$. The element size $\Delta = \lambda_e/16$ and the number of RWG unknowns is 3040.

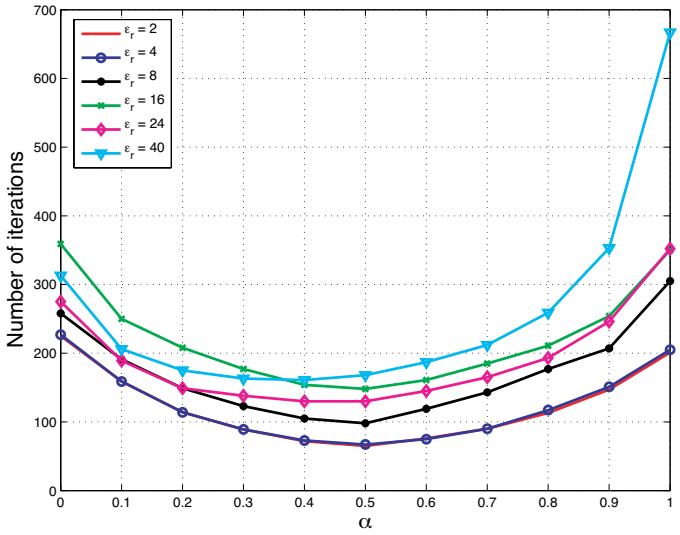

Figure 6. Number of GMRES iterations of JM-CFIE2(α) formulation similarly as in Fig. 5.

CFIE1(α) and JM-CFIE2(α) formulations using the CFIE operator

$$\begin{bmatrix} \boldsymbol{\mathcal{C}}^{\mathrm{e}}_{\alpha,1-\alpha}+\boldsymbol{\mathcal{C}}^{\mathrm{i}}_{\alpha,1-\alpha} & \frac{1}{\eta_{\mathrm{e}}}\,\boldsymbol{n}_{\mathrm{e}}\times\boldsymbol{\mathcal{C}}^{\mathrm{e}}_{1-\alpha,\alpha}+\frac{1}{\eta_{\mathrm{i}}}\,\boldsymbol{n}_{\mathrm{i}}\times\boldsymbol{\mathcal{C}}^{\mathrm{i}}_{1-\alpha,\alpha} \\ -\eta_{\mathrm{e}}\,\boldsymbol{n}_{\mathrm{e}}\times\boldsymbol{\mathcal{C}}^{\mathrm{e}}_{1-\alpha,\alpha}-\eta_{\mathrm{i}}\,\boldsymbol{n}_{\mathrm{i}}\times\boldsymbol{\mathcal{C}}^{\mathrm{i}}_{1-\alpha,\alpha} & \boldsymbol{\mathcal{C}}^{\mathrm{e}}_{\alpha,1-\alpha}+\boldsymbol{\mathcal{C}}^{\mathrm{i}}_{\alpha,1-\alpha} \end{bmatrix}\begin{bmatrix} \boldsymbol{J} \\ \boldsymbol{M} \end{bmatrix} = \begin{bmatrix} \boldsymbol{G}^{p,\mathrm{e}}_{\alpha,1-\alpha} \\ -\eta_{\mathrm{e}}\boldsymbol{n}_{\mathrm{e}}\times\boldsymbol{G}^{p,\mathrm{e}}_{1-\alpha,\alpha} \end{bmatrix} \tag{12}$$

$$\begin{bmatrix} \boldsymbol{\mathcal{C}}^{\mathrm{e}}_{\alpha,1-\alpha}+\boldsymbol{\mathcal{C}}^{\mathrm{i}}_{\alpha,1-\alpha} & \frac{1}{\eta_{\mathrm{e}}}\boldsymbol{n}_{\mathrm{e}}\times\boldsymbol{\mathcal{C}}^{\mathrm{e}}_{1-\alpha,\alpha}+\frac{1}{\eta_{\mathrm{i}}}\boldsymbol{n}_{\mathrm{i}}\times\boldsymbol{\mathcal{C}}^{\mathrm{i}}_{1-\alpha,\alpha} \\ -\eta_{\mathrm{e}}\,\boldsymbol{n}_{\mathrm{e}}\times\boldsymbol{\mathcal{C}}^{\mathrm{e}}_{\alpha,1-\alpha}-\eta_{\mathrm{i}}\,\boldsymbol{n}_{\mathrm{i}}\times\boldsymbol{\mathcal{C}}^{\mathrm{i}}_{\alpha,1-\alpha} & \boldsymbol{\mathcal{C}}^{\mathrm{e}}_{1-\alpha,\alpha}+\boldsymbol{\mathcal{C}}^{\mathrm{i}}_{1-\alpha,\alpha} \end{bmatrix}\begin{bmatrix} \boldsymbol{J} \\ \boldsymbol{M} \end{bmatrix} = \begin{bmatrix} \boldsymbol{G}^{p,\mathrm{e}}_{\alpha,1-\alpha} \\ -\eta_{\mathrm{e}}\boldsymbol{n}_{\mathrm{e}}\times\boldsymbol{G}^{p,\mathrm{e}}_{\alpha,1-\alpha} \end{bmatrix}. \tag{13}$$

In (12) and (13) $\boldsymbol{J}=\boldsymbol{J}_{\mathrm{e}}=-\boldsymbol{J}_{\mathrm{i}}$ and $\boldsymbol{M}=\boldsymbol{M}_{\mathrm{e}}=-\boldsymbol{M}_{\mathrm{i}}$ and

$$\boldsymbol{G}^{p,\mathrm{e}}_{\alpha,\beta}=-\alpha\,\frac{1}{\eta_{\mathrm{e}}}\boldsymbol{E}^{p}_{\mathrm{e}}(\boldsymbol{r})_{\tan}-\beta\,\boldsymbol{n}_{\mathrm{e}}\times\boldsymbol{H}^{p}_{\mathrm{e}}(\boldsymbol{r}) \tag{14}$$

is a combined primary (or incident) field with sources in the exterior.

Consider next the JM-CFIE1(α) formulation at $\alpha=0$. The operators of this formulation read

$$\boldsymbol{n}\times\begin{bmatrix} \boldsymbol{\mathcal{K}}_{\mathrm{e}}-\boldsymbol{\mathcal{K}}_{\mathrm{i}} & \frac{1}{\eta_{\mathrm{e}}}\,\boldsymbol{\mathcal{L}}_{\mathrm{e}}-\frac{1}{\eta_{\mathrm{i}}}\,\boldsymbol{\mathcal{L}}_{\mathrm{i}} \\ -\eta_{\mathrm{e}}\,\boldsymbol{\mathcal{L}}_{\mathrm{e}}+\eta_{\mathrm{i}}\,\boldsymbol{\mathcal{L}}_{\mathrm{i}} & \boldsymbol{\mathcal{K}}_{\mathrm{e}}-\boldsymbol{\mathcal{K}}_{\mathrm{i}} \end{bmatrix}-\Omega\begin{bmatrix} \boldsymbol{\mathcal{I}} & 0 \\ 0 & \boldsymbol{\mathcal{I}} \end{bmatrix}. \tag{15}$$

Here $\boldsymbol{n}=\boldsymbol{n}_{\mathrm{e}}=-\boldsymbol{n}_{\mathrm{i}}$ and $\boldsymbol{n}$ operates separately to each of the operators of the first matrix. Clearly (15) is an integral operator of the second kind (an integral operator plus the identity operator $\boldsymbol{\mathcal{I}}$). At $\varepsilon_{\mathrm{e}}=\varepsilon_{\mathrm{i}}$ (and $\mu_{\mathrm{e}}=\mu_{\mathrm{i}}$) the first matrix of (15) vanishes ([13]) and JM-CFIE1(0) reduces to the identity operator. Disretization of an identity operator with low order subdomain basis functions leads to a nearly identity matrix. Since the identity matrix is ideal for iterative solvers, JM-CFIE1(0) usually leads to very good iteration convergence as the permittivity and permeability of the background and the object coincide and also for sufficiently low contrast objects. As ε_{i} differs from ε_{e}, the first matrix of (15) does not vanish yielding a less diagonally dominant matrix. Eventually, as the permittivity contrast is high enough, the off-diagonal blocks of the first matrix of (15) become ill-balanced and the iteration convergence of JM-CFIE1(α) essentially slows down.

At $\alpha=1$ JM-CFIE1(α) formulation does not have a similar behavior, because the identity operator vanishes and JM-CFIE1(1)

reduces to an integral equation of the first kind. Since JM-CFIE1(α) with $\alpha = 0$ seems to be the most sensitive to the increase of the permittivity contrast (see e.g., Figure 1), we may conclude that the permittivity instability of the JM-CFIE1(α) formulation is a consequence of the properties of the integral equation of the second kind JM-CFIE1(0).

The behavior of JM-CFIE2(α) is different because it is a combination of integral equations of the first and second kind for all α, $0 \leq \alpha \leq 1$. This means that a similar argument as with JM-CFIE1(α) does not hold and the optimum α for the JM-CFIE2(α) formulation is less sensitive to the permittivity. The problem with JM-CFIE2(α) is that the two identity operators of the combined system (13) are identical only if $\alpha = 0.5$. Because the balance of the identity operators is very important for the conditioning of the integral equations of the second kind [13], and JM-CFIE2(α) contains the identity operators for all α, this explains why the choice $\alpha = 0.5$ is usually the optimal one for JM-CFIE2(α).

In the next section a method to stabilize the properties of the JM-CFIE(α) formulations with respect to the permittivity is introduced.

5. STABILIZING JM-CFIE(α) FORMULATIONS

In [19] and [16] a new idea to improve conditioning of the electromagnetic surface integral equations was proposed. This idea is based on the use of normalized fields and currents, defined as follows

$$\tilde{\boldsymbol{E}} = \sqrt{\varepsilon}\boldsymbol{E}, \qquad \tilde{\boldsymbol{H}} = \sqrt{\mu}\boldsymbol{H}, \tag{16}$$

$$\tilde{\boldsymbol{M}} = -\boldsymbol{n} \times \tilde{\boldsymbol{E}}, \quad \tilde{\boldsymbol{J}} = \boldsymbol{n} \times \tilde{\boldsymbol{H}}. \tag{17}$$

The results of [16] show that with the normalized fields and currents (16), (17) balance between the matrix elements and conditioning of the matrix of the original JM-CFIE formulation can be essentially improved. In particular, this is the case at (very) high permittivities and at (very) low frequencies. The drawback of this method is that the normalized currents are not necessarily continuous on the interfaces and special scaling factors are required to achieve continuity and maintain good balance of the matrix. In [16] three different scaling factors were proposed by defining the following $2N \times 2N$ diagonal matrices

$$\boldsymbol{S} = \mathrm{diag}\left[s_\mu, s_\varepsilon\right], \quad \boldsymbol{T} = \mathrm{diag}\left[s_\varepsilon, s_\mu\right], \quad \text{and} \quad \boldsymbol{R} = \boldsymbol{S}^{-1}, \tag{18}$$

where $s_\mu = \sqrt{\mu_{rl}}/\sqrt{\mu_{ri} + \mu_{re}}$ and $s_\varepsilon = \sqrt{\varepsilon_{rl}}/\sqrt{\varepsilon_{ri} + \varepsilon_{re}}$ are $N \times 1$ vectors and N is the number of unknowns of $\boldsymbol{J}$ and $\boldsymbol{M}$ (in the case

of a homogeneous dielectric object). Above μ_{rl} and ε_{rl}, $l = i, e$ are the relative permeability and permittivity of the interior ($l = i$) and exterior ($l = e$).

Next this idea is applied to JM-CFIE1(α) and JM-CFIE2(α). The formulations with the normalized fields and currents, and with various scaling factors, are defined as follows

$$\text{ssJM-CFIEj}(\alpha): \quad \alpha\,\text{ssJM-CFIEj}(1) + \beta\,\text{ssJM-CFIEj}(0) \tag{19}$$

$$\text{tsJM-CFIEj}(\alpha): \quad \alpha\,\text{tsJM-CFIEj}(1) + \beta\,\text{tsJM-CFIEj}(0) \tag{20}$$

$$\text{rsJM-CFIEj}(\alpha): \quad \alpha\,\text{rsJM-CFIEj}(1) + \beta\,\text{rsJM-CFIEj}(0). \tag{21}$$

Here $j = 1, 2$ and ss stands for multiplying the system matrix from left and right by matrix $\boldsymbol{S}$. Note that this multiplication is done separately in both regions [16]. Notations ts and rs are defined similarly.

Figures 7–12 show the number of GMRES iterations of the rsJM-CFIE1(α) and ssJM-CFIE2(α) formulations with RWG functions. The geometries are the same as in Section 3. The other formulations were also tested, but their accuracy and iteration counts were found to be more sensitive to the choice of α and permittivity. For some α the other formulations, however, may give lower iteration count [16].

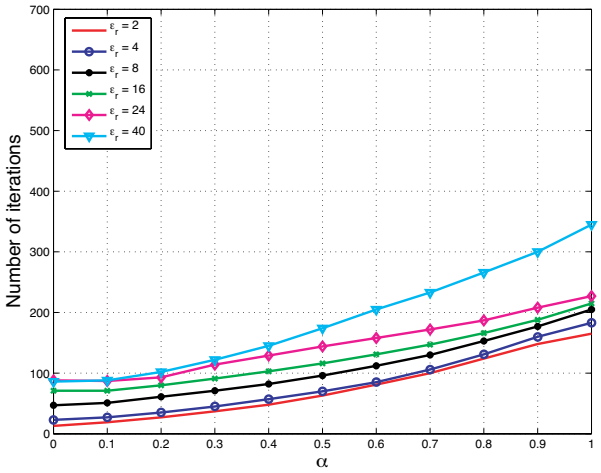

Figure 7. Number of GMRES iterations of rsJM-CFIE1(α) formulation for a dielectric cube with $\varepsilon_r = 2, \ldots, 40$ and RWG functions. Element size $\Delta = \lambda_e/20$ and the number of unknowns is 3600.

Figures 7–12 show that for the rsJM-CFIE1(α) formulation the optimal value of α minimizing the number of iterations is close to 0.1,

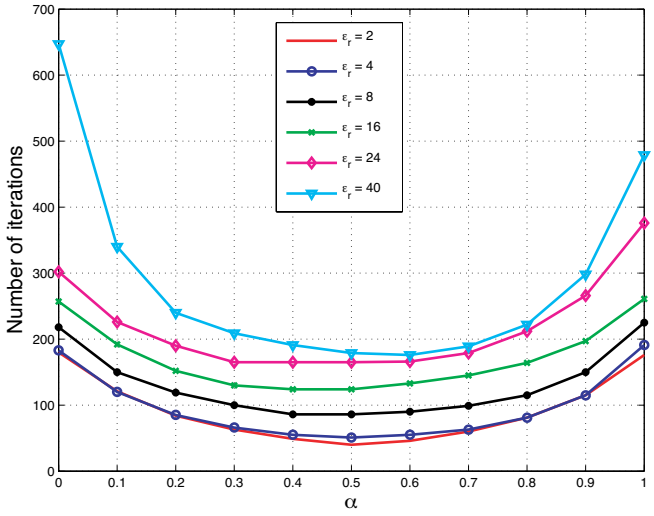

Figure 8. Number of GMRES iterations of ssJM-CFIE2(α) formulation similarly as in Fig. 7.

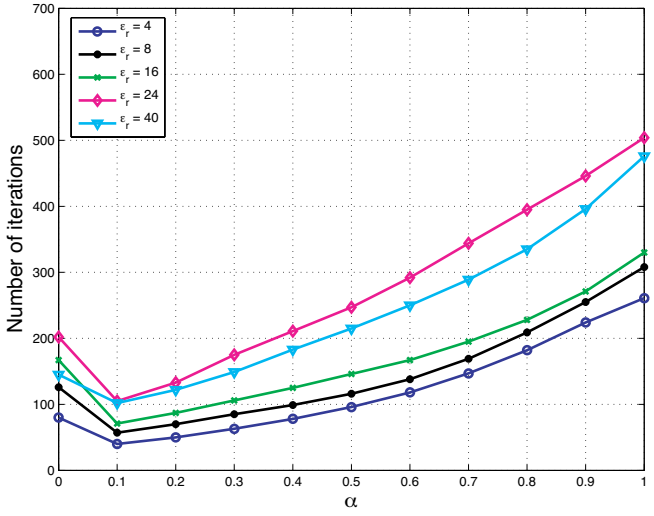

Figure 9. Number of GMRES iterations of rsJM-CFIE1(α) formulation for a piecewise homogeneous dielectric cube with $\varepsilon_{r1} = 2$, $\varepsilon_{r2} = 4, \ldots, 40$ and RWG functions. Element size $\Delta = \lambda_e/16$ and the number of unknowns is 4192.

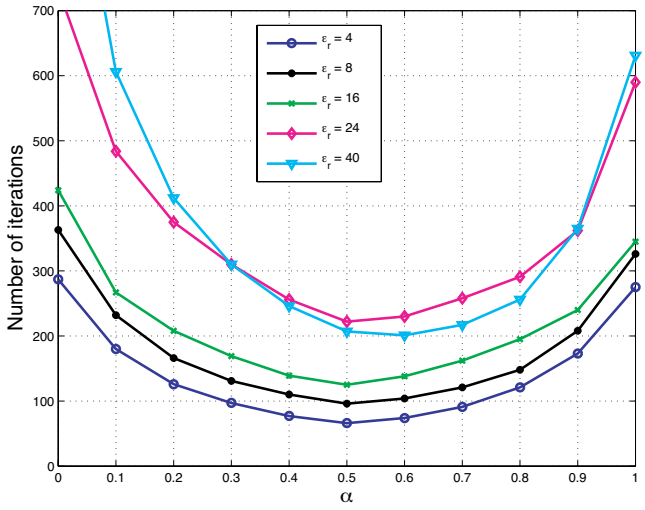

Figure 10. Number of GMRES iterations of ssJM-CFIE2(α) formulation similarly as in Figure 9.

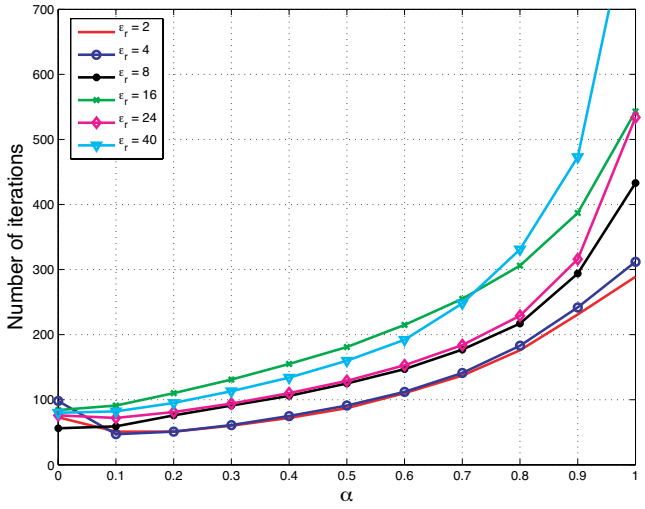

Figure 11. Number of GMRES iterations of rsJM-CFIE1(α) formulation for a composite metallic and dielectric cube with $\varepsilon_r = 2, \ldots, 40$ and RWG functions. Element size $\Delta = \lambda_e/16$ and the number of unknowns is 3040.

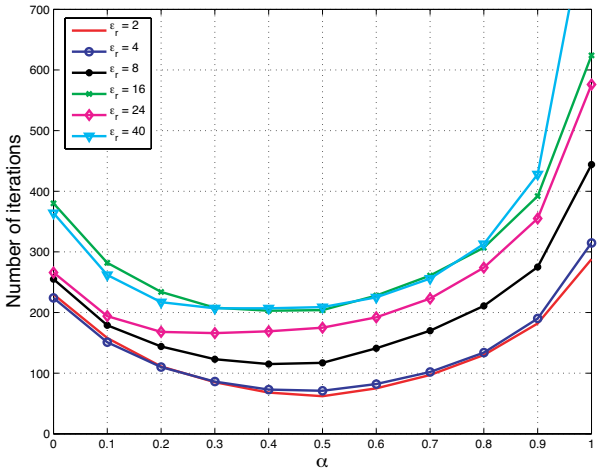

Figure 12. Number of GMRES iterations of ssJM-CFIE2(α) formulation similarly as in Fig. 11.

and for the ssJM-CFIE2(α) formulation it is close to 0.5. This seems to be true for all considered permittivities and geometries. Hence, we may conclude that by using normalized field quantities the numerical stability of the formulations with respect to the permittivity can be improved.

Next we consider the formulations more carefully. Consider first the JM-CFIE1(α) formulation. The operators of the JM-CFIE1(0) formulation with normalized fields and currents read [16]

$$\boldsymbol{n}\times\begin{bmatrix} \boldsymbol{\mathcal{K}}_{\mathrm{e}}-\boldsymbol{\mathcal{K}}_{\mathrm{i}} & \boldsymbol{\mathcal{L}}_{\mathrm{e}}-\boldsymbol{\mathcal{L}}_{\mathrm{i}} \\ -\boldsymbol{\mathcal{L}}_{\mathrm{e}}+\boldsymbol{\mathcal{L}}_{\mathrm{i}} & \boldsymbol{\mathcal{K}}_{\mathrm{e}}-\boldsymbol{\mathcal{K}}_{\mathrm{i}} \end{bmatrix}-\Omega\begin{bmatrix} \boldsymbol{\mathcal{I}} & 0 \\ 0 & \boldsymbol{\mathcal{I}} \end{bmatrix}. \tag{22}$$

Here the first operator matrix is essentially antisymmetric and hence, better balanced than in (15). This means that the conditioning of the matrix improves, in particular, at high permittivities. Note that with the additional scaling factors the operator matrix is different, but these factors are chosen so that the good balance of the operators in (22) is still maintained.

In the case of homogeneous dielectric objects theoretically $\alpha = 0$ should be the optimal choice for rs-JMCFIE1(α). There are two reasons for this. Firstly, the system is well-balanced and of the second kind. Secondly, the formulation, similarly as the Müller formulation, is a mesh and frequency stable formulation [16], meaning that as the mesh density is increased, or the frequency is decreased, the condition

number of the matrix remains bounded. It is important to note that ssJM-CFIE2(α) with any value of α and rsJM-CFIE1(α) with any other value of $\alpha(> 0)$ does not have this property. We note that the situation may be different at (very) high frequencies, as observed in [18] in the case of the Müller formulation, because rs-JMCFIE(0), similarly as the Müller formulation, usually work better at lower frequencies.

In the case of inhomogeneous objects with junctions the situation is different. In these cases the optimum α for the rsJM-CFIE1(α) formulation seems to be close to 0.1 rather than 0. The reason for this is that rsJM-CFIE1(0) does not have the Müller property [16]. This shows also, similarly as in the case of PEC objects, that generally it is advantageous to apply a CFIE type formulation with a small coupling parameter, rather than a MFIE or Müller formulation (of the second kind).

By using the normalized fields and currents the balance of the first matrix of ssJM-CFIE2(α) formulation can be improved, too. However, because this does not effect on the balance of the identity operators, ssJM-CFIE2(α) will give the lowest number of iterations as the identity operators have identical coefficients, i.e., as $\alpha = 0.5$. This agrees with numerical results and actually shows that JM-CFIE2(α) formulation does not provide any additional benefit compared to the original JM-CFIE formulation considered in [7] and [16].

6. SOLUTION ACCURACY

Another important property of a surface integral equation formulation is the accuracy of the solution. Recent studies have shown that surface integral equation formulations may have very different accuracy, see e.g., [11–14]. In particular, the choice of a formulation is important if the surface is non-smooth [12] or the material contrast is very low [17] or very high [16]. Next the solution accuracy of the JM-CFIE1(α) and rsJM-CFIE1(α) formulations is studied.

Figures 13–16 show the backscattered or forward scattered radar cross section for the same geometries as in Section 3. The equations are discretized using Galerkin's method with RWG and linear-linear (LL) basis functions [21] using different mesh densities.

The results of Figure 13 show that in the case of a homogeneous dielectric cube the solution (RCS) of JM-CFIE1(1) and rsJM-CFIE(1) converges much more rapidly than the solution of JM-CFIE1(0) and rsJM-CFIE(0) as the number of unknowns is increased. Hence, the optimum α for the solution accuracy is one, which is almost an opposite value to the optimum for the iteration convergence. This phenomenon is associated with the fundamental properties of the integral operators

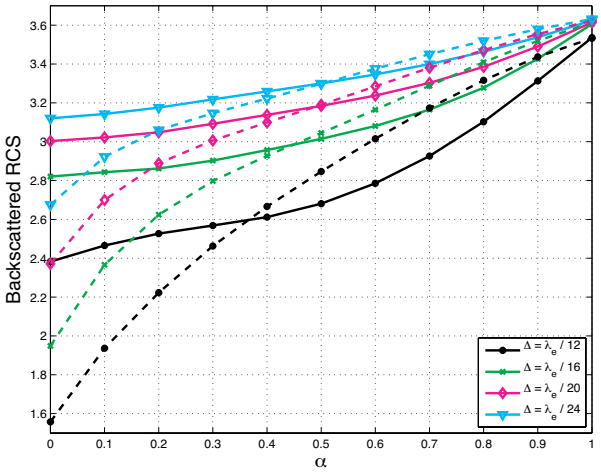

Figure 13. Backscattered RCS of JM-CFIE1(α) (solid line) and rsJM-CFIE1(α) (dashed line) formulations for a homogeneous dielectric cube with $\varepsilon_r = 24$, four different mesh densities and RWG functions. The corresponding numbers of unknowns are 1296, 2304, 3600 and 5184.

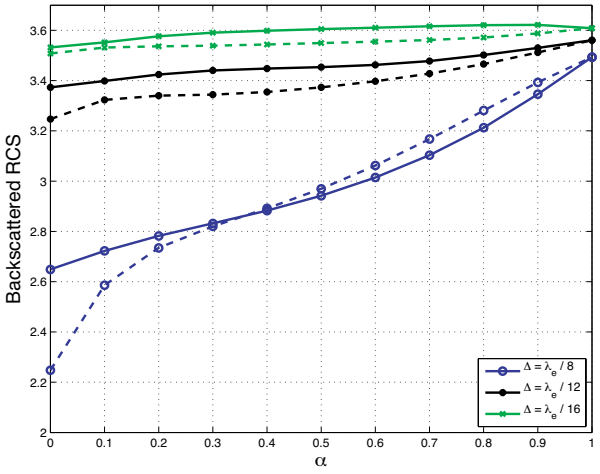

Figure 14. Backscattered RCS of JM-CFIE1(α) (solid line) and rsJM-CFIE1(α) (dashed line) formulations for a homogeneous dielectric cube with $\varepsilon_r = 24$, three different mesh densities and LL functions. The numbers of unknowns are 1152, 2592 and 4608.

and to their singularity, and is discussed in detail in [12].

Figure 14 shows the results for a homogeneous cube with LL functions. If the mesh density is fine enough, the solution accuracy with LL functions is less sensitive to the choice of α than with RWG functions. In particular, the solution accuracy of JM-CFIE1(0) and rsJM-CFIE1(0) formulations improve significantly. A similar phenomenon has been observed previously in the case of PEC-CFIE [11]. In comparing the results with the RWG and LL functions it is important to remember that for the same mesh the LL functions double the number of unknowns compared to the RWG functions. Figures 15–18 show the same results for inhomogeneous objects. In Figures 13–18 curves with the same markers correspond to the same element size.

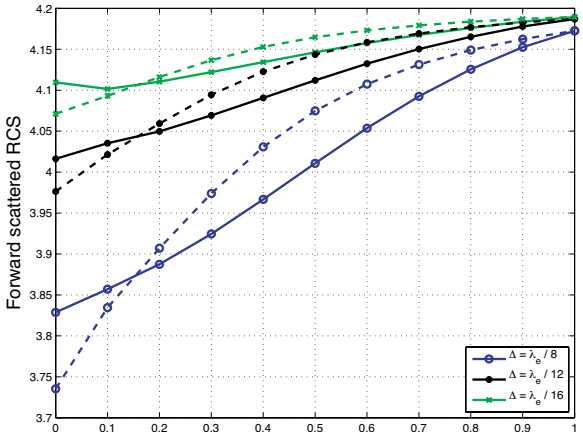

Figure 15. Forward scattered RCS of JM-CFIE1(α) (solid line) and rsJM-CFIE1(α) (dashed line) formulations for a piecewise homogeneous dielectric cube with $\varepsilon_{r1} = 2$, $\varepsilon_{r2} = 24$, three different mesh densities and RWG functions. The numbers of unknowns are 1040, 2352 and 4192.

Figures 17 and 18 show another interesting result. In the case of composite metallic and dielectric objects with junctions and sharp wedges, the solution accuracy of JM-CFIE1(α) and rsJM-CFIE1(α) formulations with small values of α (between 0 and 0.1) is very sensitive to the mesh density. This phenomenon has been identified as a general accuracy problem of the integral equations of the second kind at sharp metallic (or dielectric) wedges and corners [12].

Next the solution accuracy of the rsJM-CFIE1(0.1) formulation is studied more carefully. Figure 19 shows the backscattered RCS as a

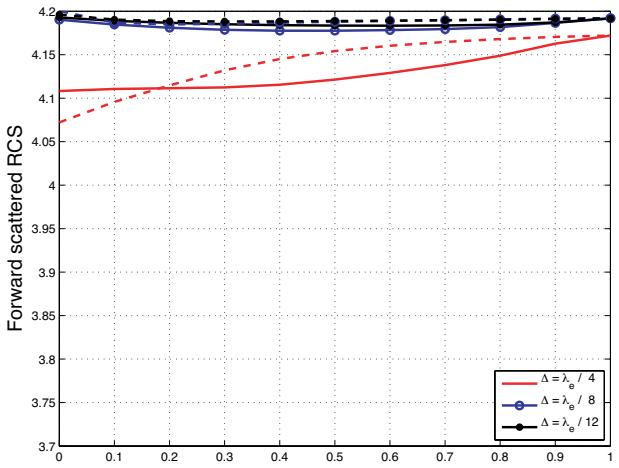

Figure 16. Forward scattered RCS of JM-CFIE1(α) (solid line) and rsJM-CFIE1(α) (dashed line) formulations for a piecewise homogeneous dielectric cube with $\varepsilon_{r1} = 2$, $\varepsilon_{r2} = 24$, three different mesh densities and LL functions. The numbers of unknowns are 512, 2080 and 4704.

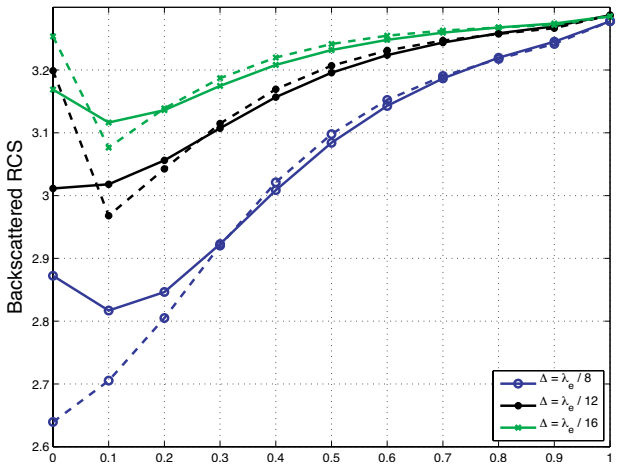

Figure 17. Backscattered RCS of JM-CFIE1(α) (solid line) and rsJM-CFIE1(α) (dashed line) formulations for a composite metallic and dielectric cube with $\varepsilon_r = 4$, three different mesh densities and RWG functions. The numbers of unknowns are 752, 1704 and 3040.

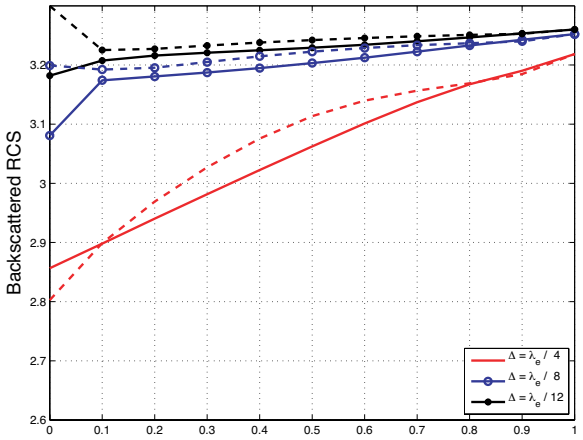

Figure 18. Backscattered RCS of JM-CFIE1(α) (solid line) and rsJM-CFIE1(α) (dashed line) formulations for a composite metallic and dielectric cube with $\varepsilon_r = 4$, three mesh densities and LL functions. The numbers of unknowns are 368, 1504 and 3408.

function of the number of unknowns. Here, in addition to the RWG and LL functions, also the second order quadratic-quadratic (QQ) functions [1] are used to discretize the equations. For comparison also the solution obtained with the integral equation of the first kind EFIE-PMCHWT formulation (EFIE on the metallic surface and PMCHWT on the dielectric interface) is plotted. EFIE-PMCHWT formulation is expected to give the fastest solution convergence (but poorest iteration convergence) [12].

Finally, the same analysis is repeated as the PEC box reduces to an open PEC plate. It is still possible to apply CFIE formulation with any α between 0 and 1 on the open PEC plate, because the plate is at an interface of two homogeneous domains with different material parameters and the currents on the opposite sides of the plate have to be considered as independent unknowns. This is an important difference compared to the case where an open PEC in a homogeneous medium and the currents on the opposite sides of the plate have to be combined and, for example, MFIE can not be used [1]. Figure 20 shows the forward scattered RCS as a function of the number of unknowns with RWG, LL and QQ functions.

Figures 19 and 20 show that the solution accuracy of rsJM-CFIE1(0.1) converges as the number of unknowns is increased and the convergence is faster with the higher order basis functions. However, the convergence is always poorer than with the EFIE-PMCHWT

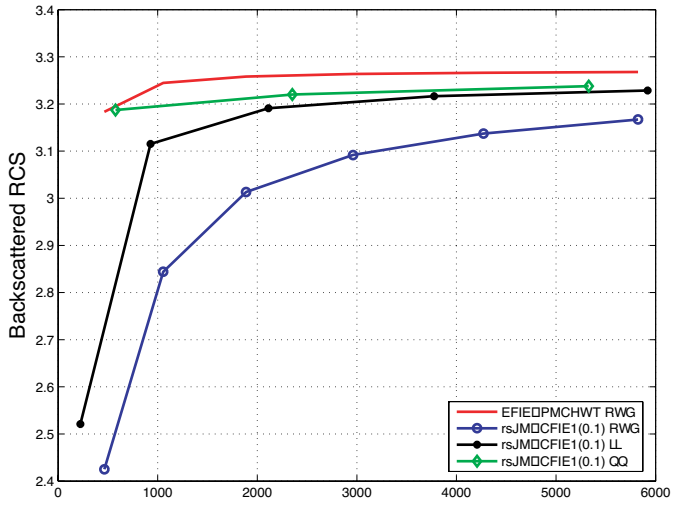

Figure 19. Backscattered RCS of rsJM-CFIE1(0.1) as a function of the number of unknowns for a composite metallic and dielectric cube ($\varepsilon_r = 4$) with RWG, LL and QQ functions.

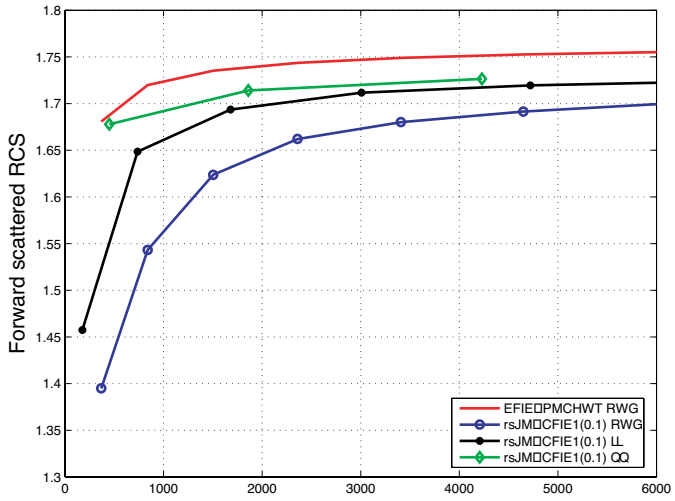

Figure 20. Backscattered RCS of rsJM-CFIE1(0.1) as a function of the number of unknowns for a dielectric box ($\varepsilon_r = 4$) with an open PEC plate, similarly as in Figure 19.

formulation and RWG functions. Finally we note that in the last example case the number of iterations behave rather similarly as in Figure 11.

7. CONCLUSIONS

The previously developed JM-CFIE formulation for homogeneous dielectric and composite metallic and dielectric objects [7] is generalized by adding a similar coupling parameter α as CFIE contains in the case of PEC objects. Two alternative JM-CFIE(α) formulations, JM-CFIE1(α) and JM-CFIE2(α), are presented and their numerical properties (solution accuracy and convergence of iterative solutions) are investigated.

Numerical experiments show a major difference between the PEC-CFIE and the dielectric CFIE (JM-CFIE1(α) and JM-CFIE2(α)). In the dielectric case the optimal value of α minimizing the number of iterations may depend strongly on the permittivity of the object. By using normalized fields and currents [16] the behavior of the new JM-CFIE(α) formulations can be stabilized and the optimum α minimizing the number of iterations becomes nearly independent on the permittivity. In addition, if linear-linear functions instead of the more conventional constant-linear RWG functions are used to discretize the equations, the solution accuracy becomes less dependent on the choice of α.

In the first form of the new JM-CFIE(α) formulations, JM-CFIE1(α), the normalized fields and currents are required to stabilize the behavior of the formulation at $\alpha = 0$. Since JM-CFIE1(0) is an integral equation of the second kind, the same technique could be used to stabilize other integral equations of the second kind with respect to the permittivity, or with some other parameter, too. After the stabilization, the optimum α for the iteration convergence seems to be near 0.1.

In the second form of the new JM-CFIE(α) formulations, JM-CFIE2(α), the use of normalized fields and currents is less significant. In most cases the optimum α for JM-CFIE2(α), and its stabilized version, is 0.5. Since $\alpha = 0.5$ corresponds to the original JM-CFIE formulation presented in [7] and [16], JM-CFIE2(α) does not provide any significant benefit compared to the original one.

The numerical experiments show that in the most cases the stabilized version of the new JM-CFIE1(α) formulation with $\alpha = 0.1$, i.e., rsJM-CFIE1(0.1), gives the lowest iteration count. For low permittivities, however, JM-CFIE1(0.1) with conventional fields and currents leads to almost the same number of iterations. In order to

obtain accurate solutions with rsJM-CFIE1(0.1) and JM-CFIE1(0.1) at least linear-linear basis functions are required in the discretization. For non-smooth metallic objects or non-smooth dielectric objects with high permittivities, higher order basis functions may be required to maintain the solution accuracy. This is a consequence of a general accuracy problem of the integral equations of the second kind.

ACKNOWLEDGMENT

This work is supported by the Academy of Finland, Grant number 108801.

REFERENCES

1. Kolundzija, B. M. and A. R. Djordjevic, *Electromagnetic Modeling of Composite Metallic and Dielectric Structures*, Artech House, Boston, 2002.
2. Mautz, J. R. and R. F. Harrington, "H-field, E-field and combined-field solutions for conducting bodies of revolution," *Arch. Elektr. Übertragung.*, Vol. 32, 157–164, 1978.
3. Mautz, J. R. and R. F. Harrington, "Electromagnetic scattering from a homogeneous material body of revolution," *Arch. Elektron. Übertragungstechn. (Electron. Commun.)*, Vol. 33, 71–80, 1979.
4. Rao, S. M. and D. R. Wilton, "E-field, H-field, and combined field solution for arbitrarily shaped three-dimensional dielectric bodies," *Electromagnetics*, Vol. 10, 407–421, 1990.
5. Sheng, X.-Q., J.-M. Jin, J. Song, W. C. Chew, and C.-C. Lu, "Solution of combined-field integral equation using multilevel fast multipole algorithm for scattering by homogeneous bodies," *IEEE Trans. Antennas Propag.*, Vol. 46, No. 11, 1718–1726, Nov. 1998.
6. Jung, B. H., T. K. Sarkar, and Y.-S. Chung, "A survey of various frequency domain integral equations for the analysis of scattering from three-dimensional dielectric objects," *Progress In Electromagnetic Research*, PIER 36, 193–246, 2002.
7. Ylä-Oijala, P. and M. Taskinen, "Application of combined field integral equation for electromagnetic scattering by composite metallic and dielectric objects," *IEEE Trans. Antennas Propag.*, Vol. 53, No. 3, 1168–1173, March 2005.
8. Jung, B. H. and T. K. Sarkar, "Analysis of scattering from arbitrarily shaped 3-D conducting/dielectric composite objects

using a combined field integral equation," *J. of Electromag. Waves and Applicat.*, Vol. 18, No. 6, 729–743, June 2004.

9. Jung, B. H., T. K. Sarkar, and M. Salazar-Palma, "Combined field integral equation for the analysis of scattering from three-dimensional conducting bodies coated with a dielectric material," *Microwave Opt. Technol. Lett.*, Vol. 40, No. 6, 511–516, March 2004.
10. Song, J. M. and W. C. Chew, "Multilevel fast multipole algorithm for solving combined field integral equations of electromagnetic scattering," *Microw. Opt. Technol. Lett.*, Vol. 10, No. 1, 14–19, Sep. 1995.
11. Ergül, Ö. and L. Gürel, "Improving the accuracy of the magnetic field integral equation with the linear-linear basis functions," *Radio Science*, Vol. 41, RS4004, 2006.
12. Ylä-Oijala, P., M. Taskinen, and S. Järvenpää, "Analysis of surface integral equations in electromagnetic scattering and radiation problems," *Engineering Analysis with Boundary Elements*, Vol. 12, 196–209, 2008.
13. Ylä-Oijala, P., M. Taskinen, and S. Järvenpää, "Surface integral equation formulations for solving electromagnetic scattering problems with iterative methods," *Radio Science*, Vol. 40, No. 6, RS6002, Nov. 2005.
14. Zhu, A., S. Gedney, and J. L. Visher, "A study of combined field formulations for material scattering for a locally corrected Nyström discretization," *IEEE Trans. Antennas Propag.*, Vol. 53, No. 12, 4111–4120, Dec. 2005.
15. Lloyd, T. W., J. M. Song, and M. Yang, "Numerical study of surface integral formulations for low-contrast objects," *IEEE Antennas and Wireless Propagation Letters*, Vol. 4, 482–485, 2005.
16. Ylä-Oijala, P. and M. Taskinen, "Improving conditioning of the electromagnetic surface integral equations using normalized field quantities," *IEEE Trans. Antennas Propag.*, Vol. 55, No. 1, 178–185, Jan. 2007.
17. Ergül, Ö. and L. Gürel, "Accurate solutions of scattering problems involving low-contrast dielectric objects with surface integral equations," *Proceedings of the Second European Conference on Antennas and Propagation, EuCAP 2007*, 390, Edinburgh, Nov. 2007.
18. Ergül, Ö. and L. Gürel, "Fast and accurate solutions of scattering problems involving dielectric objects with moderate and low contrasts," *Proceedings of 2007 Computational Electromagnetics*

Workshop, CEM'07, 59–64, Izmir, Turkey, August 30–31, 2007.

19. Taskinen, M. and P. Ylä-Oijala, "Current and charge integral equation formulation," *IEEE Trans. Antennas Propag.*, Vol. 54, No. 1, 58–67, Jan. 2006.
20. Rao, S. M., D. R. Wilton, and A. W. Glisson, "Electromagnetic scattering by surfaces of arbitrary shape," *IEEE Trans. Antennas Propag.*, Vol. 30, No. 3, 409–418, 1982.
21. Trintinalia, L. C. and H. Ling, "First order triangular patch basis functions for electromagnetic scattering analysis," *Journal of Electromagnetic Waves and Applications*, Vol. 15, No. 11, 1521–1537, 2001.